Journal of Structural Engineering and Geotechnics,

12(1), 75-85, Winter & Spring 2022

Numerical Investigation of the limit equilibrium method in Tunnel Stability Using Finite Element (FEM)

Semko Arefpanah [a,*], Alireza Sharafi [a]

Department of Civil Engineering, Science and Research Branch، Islamic Azad University, Tehran, Iran

Received 27 July 2022, Accept 17 January 2023

Abstract

The upper bound solution of the factor of safety is obtained by optimization calculation. In this paper, a new method for tunnel stability analysis is proposed, that is, the external force increment method is used to convert the stability ratio of traditional tunnels. Evaluating the feasibility of the method proposed in this paper, it was compared with the safety factor calculated by the marginal equilibrium method. To evaluate the feasibility of the method proposed in this paper, it was compared with the safety factor calculated by the marginal equilibrium method. Two newly defined parameters: one normal stability ratio and the critical stability ratio. Can be defined as the field stability ratio, which consists of two newly de fined parameters, namely the natural stability ratio and the critical stability ratio. Therefore when the initial tunnel is stable or unstable, the relationship between the electric field stability ratio and the critical stability ratio is determined. The sta bility of the tunnel surface is estimated by the upper limit theorem of the limit analysis together with the strength reduction technique by the safety factor widely used in the slope stability analysis. There are two methods to reach the critical steady state by increasing the tunnel according to the field stabilization factor. One is to calculate external work (increase the external load) and the other is internal energy dissipation in a kinematically acceptable velocity field (decrease the internal load). The tunnel-bearing capacity relationship is arranged to reach the critical stability ratio of the two external force enhancement methods. In this way, the upper limit solutions of single tunnels, twin tunnels of the same diameter, and twin tunnels of different diameters are analyzed. The tunnel stability ratios were obtained by the external force increment method (EFI). Parametric studies showed that the parameters m and C/D have a significant influence on the FOS stabilization of the tunnel. As a result of the comparison, the solutions derived from these two methods agree well with each other, so the method proposed in this paper can be considered effective.

Keywords: Stability Ratio, Critical State, External Force, Safety Factor, Limit Equilibrium Method, MIDAS/GTS.

1. Introduction

Tunnel stability problems are statically uncertain, and researchers can use a variety of analytical methods. Broms et al. performed several field observations and laboratory extrusion tests in undrained clay and obtained some stability ratios (N) for openings [1]. If the stability ratio was greater than 6, the opening was considered to be unsafe which 6 being the critical stability number N_c. Using a centrifuge test, Kimura et al. gave a critical stability ratio (N_c) between 3 and 9 for shallow tunnels [2]. The critical stability ratio (N_c) is related to the geometry of the unlined tunnel heading ratio (P/D) and depthratio (C/D). Davies et al. calculated some stability ratios for shallow subsurface openings in undrained clays based on the upper bound method (UBM) and lower bound method (LBM) of limit analysis theory [3]. Square and rectangular tunnels were studied by Wilson and Abu et al [4]. Abbo et al. developed the collapse of openings in underground walls in anisotropic and heterogeneous clays, obtaining some stability ratios [5]. Ukritchon et al. used FEA Plaxis to study the 3D undrained stability of tunnel faces in heterogeneous clay [6]. This problem was investigated using Broms and Bannermark's stability number (N) according to the shear strength reduction technique. Then Safety factors for different depth ratios and designed stability ratios were calculated by the correlation equation Shiau and colleagues have developed and used the 3D FELA method, which is a stability number for circular tunnel stability with (Include c-φ) soil [7-10]. The strength reduction method (SRM) by

*Corresponding Author: Email Address: Semko.Arefpanah@srbiau.ac.ir

finite element analysis was used for slope stability analysis as early as 1975 by Sienkiewicz et al. [11], later in slope stability analysis, the strength reduction technique is used to obtain the factor of safety [12]. However, the strength reduction technique can solve the factor of the safety of slopes. The factor of safety solved is currently from slope stability condition [13]. The stability ratio of tunnels is obtained from the equilibrium condition. The stable state for the tunnels at this moment is a critical state between the tunnel stability and collapse. There are many variables in the stability number for tunnel stability analysis, and a stable state for the tunnels is hardly attained in the practice. A new analysis method, the external force increment method (EFIM) is proposed in the tunnel stability analysis [14]. That is, the stability ratio of the tunnel is detected, and when the load (soil weight, surface overload, or retaining force in the tunnel) is changed to reach the critical state of tunnel collapse [15]. This method should be more direct so that the results are according to the tunnel stability ratio equation. Therefore, to understand the tunnel collapse, several new parameters, such as field stability ratio (N_f), natural stability ratio (N_n), and critical stability ratio (N_c), are assumed. The tunnel stability plane and tunnel stability analysis plot are constructed. This research establishes the connection between the stability ratio and the factor of safety (FOS) [16]. One tunnel, two tunnels with the same diameter, and two tunnels with different diameters were analyzed by increasing the external force.

2. Upper Bound Theorem

The shear strength reduction technique was proposed by Bishop, the key point being the reduction of the soil shear strength parameter until the soil is broken. To achieve this reduction, an important concept, the shear strength reduction factor FS, is introduced. By dividing the actual shear strength parameters c and ϕ by the shear strength reduction factor, the ground strength parameters cf and ϕf used in the upper limit analysis are obtained. While the shear strength reduction factor FS gradually increased, the newly decreased soil strength parameter was obtained. The iterative process continues until a failure occurs [17]. The upper bound method is based on the calculation of strain energy. This method requires the calculation of the velocity field. This approach was commonly used in the 1960s and 1970s of the last century but was later replaced by FEM. However, this method has several advantages that make it possible to formulate efficient optimization tasks for industrial processes. The upper bound approach was first formulated by Xie J et al [18]. The upper bound theorem is used in intensity reduction techniques to control the convergence of iterative tasks. The upper bound theorem states that when the velocity boundary condition is satisfied, the load derived by equating the rate of external work to the rate of energy dissipation in any kinematically acceptable velocity field is not less than the actual collapse load. Therefore, by introducing the reduced soil strength parameter into the energy dissipation calculation, the shear strength reduction factor can be obtained based on the relationship between the external power and the energy dissipation rate [19]. Where ϕ_t is a tangential frictional angle and ct is the intercept of the straight line on the τ-axis. ϕ_t is regarded as a variable to calculate the rate of external work and energy dissipation. Using sequential quadratic programming, the upper bound solution of the objective function and the corresponding value of ϕ_t are obtained [20].

$$c_f = {}^{C}\!/_{F_s} \tag{1}$$

$$\phi_f = \arctan\left[\tan {}^{\phi}\!/_{F_s}\right] \tag{2}$$

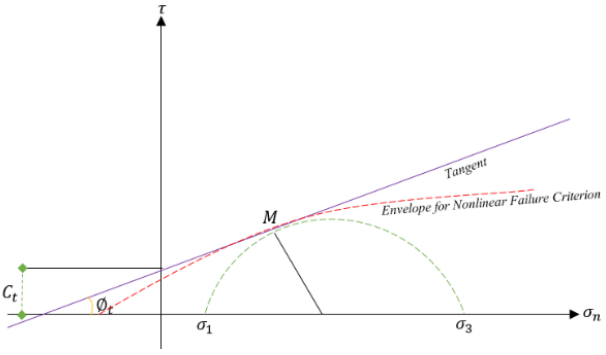

Fig. 1. Generalized tangential technique for a nonlinear failure criterion

Since the resistance range of this nonlinear failure criterion is curvilinear, the resistance parameters of the geotechnical material cannot be determined like the Mohr-Coulomb linear failure criterion. To

overcome these problems, Yang and Yin proposed a generalized tangent technique that uses the tangent in the nonlinear failure criterion at point *M* to determine the strength parameter [21].

3. Tunnel Stability Analysis Method

3.1. Basic Assumptions

It is assumed to behave consistently throughout the soil as a Tresca material with uniform undrained shear strength. For a practical tunnel in the field, based on the actual values of the parameters σ_s, σ_t, H, and C_u, the stability ratio N is obtained by using the equation:

$$N = (\sigma_s - \sigma_t + \gamma H) / C_u \quad (3)$$

Equation (3) is not a stability ratio corresponding to collapse. The stability ratio of tunnel collapse is critical N_c. A collapse stability ratio N_n needs to obtain, therefore, to investigate the stability state of a tunnel, the stability ratio can be regarded as a criterion. To facilitate the solution, equation (3) is transformed as follows:

$$N_f = (1/C_u) \sum \sigma + N_n \quad (4)$$

Where N_f is field stability ratio, critical stability ratio (N_c) = field stability ratio (N_f) when a tunnel collapses; N_n is the natural stability ratio which is equal to $\gamma H/C_u$; $\Sigma\sigma$ is the difference for $(\sigma_s - \sigma_t)$ in equation (1) between surface pressure and tunnel support pressure.

If only N_f is known, whether the tunnel is in a stable or in a collapsed state, which is unable judged. So, the computed result with the collapse stability ratio of the tunnel is very necessary to compare. A useful plot can be established for tunnel stability analysis by equation (4). A principal type is shown as follows in Figure 2.

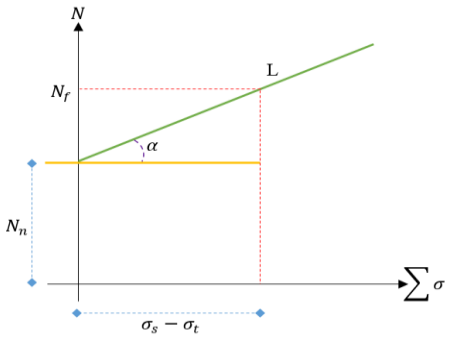

Fig. 2. Stability analysis plot

The horizontal axis represents the total external force on the surface and the tunnel lining, and the vertical axis represents the stability ratio in Fig. 2. The straight-line 'L' is defined as a "STABILITY ANALYSIS LINE" (SAL). The stability ratios of the tunnel will lie on SAL. The value of the natural stability ratio N_n is the intersection point at which the SAL line meets the vertical axis, which shows that only the soil weight acts on the tunnel and influences its stability state. The total force $(\sigma_s - \sigma_t)$ is zero. N_f in the plot is a field stability ratio. N_f has three possible values: larger than, smaller than, and equal to the critical stability ratio (N_c) of a tunnel. An angle is equal to $\tan^{-1}(1/C_u)$ which is usually a small value. The key procedure in tunnel collapse analysis is how to obtain the critical stability ratio (N_c) according to the FEM technique.

3.2. Stability Analysis Plane

To describe the analysis procedure of searching for critical stability ratio for tunnels, we may define the first part on the right of equation (3) as the external stability ratio $N_e = (\sigma_s - \sigma_t)/C_u$. Therefore, a stability analysis plane can be created in three-dimensional coordinates as follows:

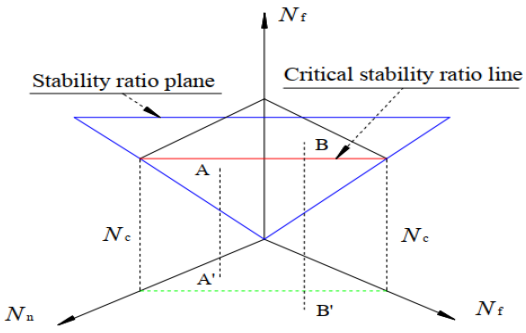

Fig.3. Stability analysis plane

The horizontal axes are N_e and N_f, and the vertical axis is N_f. A critical stability ratio line, $N_f = N_c$, is on the stability ratio plane. The collapse bound is a virtual line on N_e—N_n plane. The fieldstability ratio is a function of the natural stability ratio and external stability ratio, i.e. $N_f(N_e, N_n)$, N_f may be located to the right or left side of the collapse bound. Because the tunnel roof blowout caused by pressured air is not included in this research project ($N_e \geq 0$), all N_f values should be located on the stability analysis plane. The medium containing the tunnels is assumed to be either weightless soil or soil with self-weight ($N_e \geq 0$). Points A and B on the stability ratio plane are the initial stability ratios. They are below and above the stability ratio line,respectively. There are two cases: The initial state of the tunnel is stable ($N_f < N_c$) and the initial state of the tunnel is unstable ($N_f > N_c$).

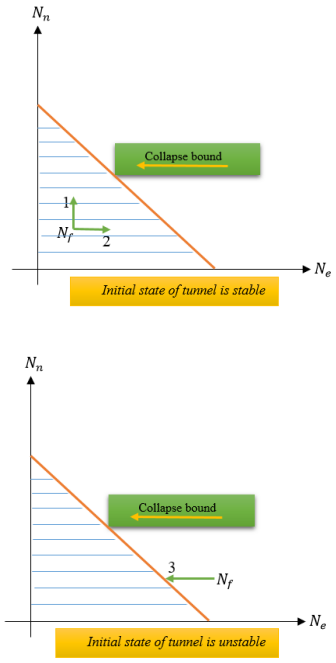

Fig. 4. Two positions of Nf on the Ne—Nn plane

In Figure 4, N_f is at the left side of the collapse bound (point in Figure 4). To obtain a collapse stability ratio, we need to increase the external stability ratio N_e (from horizontal direction 1) or increase the natural stability ratio N_n (from vertical direction 2). In Figure 4, the field stability ratio is at the right of the collapse bound (point in Figure 3) or on the collapse bound. This means that the initial state of the tunnel is unstable ($N_f \geq N_c$). When the field stability ratio is at the right of the collapse bound, to obtain a collapse stability ratio, we need to reduce the external stability ratio N_e (from the horizontal direction 3).

3.2. The criterion of Tunnel Collapse

The analysis is employed for the finite element geotechnical software package MIDAS/GTS. The Tresca model is widely used to model the undrained behavior of soil. It assumes that a material fails when the maximum shear stress at a point exceeds the limit stress (k). The limit stress parameter is further a function of the hardening parameter and is determined from experiments. Assuming that the soil around the tunnel (Maximum shear stress) is an undrained cohesive material and obeys the Tresca criterion, the elastic perfectly plastic model was used for the tunnel's stability analysis. MIDAS/GTS checks the equilibrium for internal stresses and external loads at the in situ stage and at the end of each load increment. In case the equilibrium is not satisfied, an error will lead to in situ stages. Global iterative solution based on the Full NEWTON-RAPHSON METHOD[1]. Two convergence criteria are used. They are the displacement norm method and the force norm method. Check the displacement convergence criteria using the following relationships:

$$\left|\Delta u_i\right|_2 \Big/ \left|u_i\right| \leq e_d \qquad (5)$$

Where Δu_i is displacements of the current iteration, u_i is total displacements up to the end of the current iteration, e_d is a specified tolerance. The force convergence criterion is checked using the following relationship:

$$\left|\Delta \psi_{iter}\right|_2 \Big/ \left|P\right|_2 \leq e_f \qquad (6)$$

Where $\Delta\psi_{iter}$ is the force residuals for the current iteration, P is the applied loading for the current increment, e_f is a specified tolerance. When these relationships are not satisfied, a residual force is applied in the next iteration, and so on. The maximum number of iterations is usually specified

[1] A method of convergence towards the solution by the tangent stiffness of the load-displacement diagram during the iterative analysis process

and, if reached, is assumed to be non-convergent due to the collapse of the material critical stability ratio.

Table 1.
Engineering parameters used in geotechnical designs

Description	Depth	K_0	E	φ_{cu}	C	W	γ
	m	-	Mpa	Deg	kg/cm^2	%	kN/m^3
GC/SC	0 – 5	0.41	68	25.5	0.25	3.9	17.5
SC/CL	5 – 10	0.52	30	21.25	0.3	14.5	15.5
GC/SM	10 – 15	0.41	129	25.5	0.15	16.5	16.8
GC/SC	15 – 20	0.4	120	27.2	12.8	17	20
C_u	Undrained shear strength kPA		100	Undrained shear strength from direct shear test kPA			80

3.3. Soil-structure Interaction

In general, "ground-structure interaction" refers to all analytical models in which the behavior of the ground is closely related to and meaningfully interacts with the behavior of structural members. Soil behavior is characterized by ground reaction forces, distribution, and associated ground deformation. Common load-bearing structures affected by soil-structure interactions include strip foundations, retaining walls, foundation frames, indeterminate bridge structures, and tunnel linings. The interaction of the tunnel with its surrounding environment depends on the difference between the hardness of the tunnel and the hardness of the surrounding environment. If the tunnel and the medium have the same stiffness, the displacement response of the tunnel is the same as the free field response of the medium. However, the difference between the hardness of the tunnel and the environment causes tension in the tunnel lining and there will be tunnel-environment interaction. The different modules are related to each other via Poisson's ratio. A general relationship and value for Young's modulus and Poisson's ratio can be found in Behnen et al [22]. For elastic-plastic and nonlinear elastic models of ground behavior, see relevant literature such as "Geotechnical Engineering Handbook" [23].

3.4. Geotechnical Parameters Used in the Study

Specification Geotechnical of different layers based on the information obtained from drilling boreholes near the intersection, including the depth of existing layers, specific gravity (γ), Water content (w), Cohesion (c), friction angle (φ), modulus of elasticity (E). And at-rest earth pressure coefficient (K_0) is presented in table one. The underground water level is 20 meters below the surface of the earth. The soil shear strength can be obtained using laboratory and field tests. The studies to determine the undrained shear strength were carried out by the laboratory method and then compared with the results obtained from the SPT experimental relationships. The parameters of shear strength obtained for fine-grained soils in the laboratory were determined using an undrained Cu reinforced triaxial test and undrained direct shear.

4. External Force Increment Method

Whether the initial field stability ratio is larger or smaller than the critical stability ratio, we are always able to find out the critical stability ratio with a stability analysis pot and a correct process according to the stability states. These two situations will be discussed using the stability analysis plot as follows: When $N_c > N_f$, The tunnel is stable initially. There are three alternatives to searching the critical stability ratio using the stability analysis plot.

4.1. Increasing the Unit Weight of Soil

The stability line L moves up until the stability ratio N_c is found. A new stability line 'L' is above L. N_c is on line 'L'. This situation is shown in Figure 5.

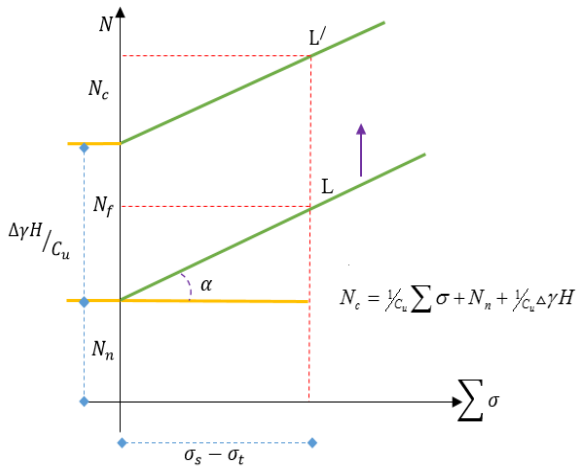

Fig.5. Nf >Nc, increase Δγ

4.2. Increasing the Surcharges on the Ground Surface

The expression of this process is that N_c is approached along the stability analysis line L from N_f until arriving at N_c in Figure 6.

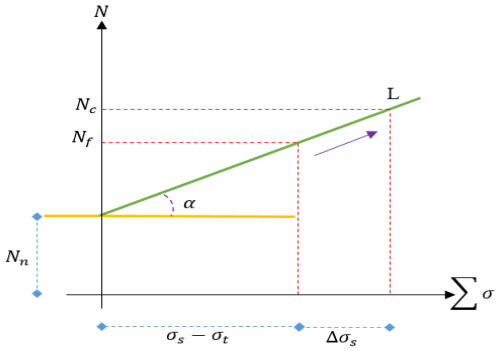

Fig. 6. $N_f < N_c$, increase $\Delta\sigma_s$

4.3. Reducing the Support Force T in the Tunnel

The procedure in this analysis is moving along line L, as shown in Figure 7, reducing the support force in the tunnel until the tunnel collapses.

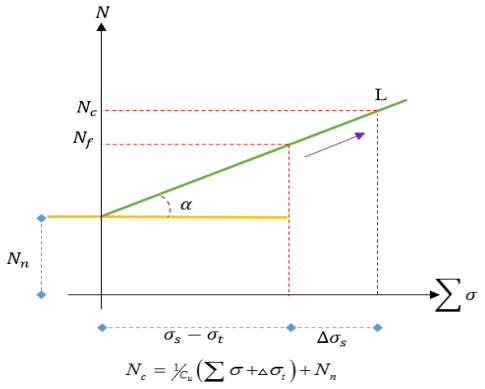

Fig. 7. $N_f < N_c$, decrease $\Delta\sigma t$

When the support force in the tunnel is reduced, the total force acting on the tunnel system is $[\sigma_s - (\sigma_t - \Delta\sigma_t)]$, which the same is as $(\Sigma\sigma + \Delta\sigma_t)$.

5. The Relationships between Stability Rabo and Factor of Safety

To evaluate the validity of the method proposed in this work, the FOS of the tunnel face is calculated by the limit equilibrium method and the upper bound theorem with the shear strength reduction technique. Numerical results for these two methods with different parameters are presented and compared with each other. Based on the silo theory, a three-dimensional failure mode of the tunnel face composed of wedges, as shown in Figure 1, is proposed by Anagnostou and Kovari [24] in the ´ framework of the limit equilibrium method. According to Bishop, the FOS for slope can be defined as the ratio of the available shear strength of the soil to that required to maintain equilibrium. Therefore, the FOS of the tunnel face derived from the wedge model presented in Figure 8 is expressed as follows:

$$FOS = {}^{N_c}\!/_{N_f} \tag{7}$$

In this study, we use the failure mechanism proposed by Leca and Dormieux to calculate the external working rate and energy dissipation rate in the framework of the upper bound theorem of the limit analysis [25]. As Leca and Dormieux have computed the rate of external work P_e ad D the tunnel diameter, γ is the unit weight of the soil $\emptyset$ is the friction angle of the soil, σs is surcharge loading, V is the velocity of the conical block, α is the angle between symmetry axis of conical block and the center line of the tunnel, and the parameters R_A, R_B, R_C are It will be written as follows. Moreover, the rate of energy dissipation produced in a kinematically acceptable velocity field is where c is the cohesive force of the soil. Based on the upper limit theorem, the expression of the holding pressure σ_T is obtained by equating the velocity of external work with the velocity of energy dissipation.

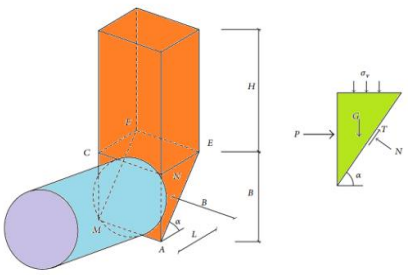

Fig. 8. Wedge stability model of tunnel face proposed by Anagnostou and Kovari

$$P_e = \frac{\pi D^2}{4}\left[-\frac{R_B R_C^2}{\cos\phi}\sigma_s - \frac{1}{3}\sin\alpha\frac{\left({}^{R_B R_C}\!/_{\sin\alpha}\right)^3 - \left({}^{R_A}\!/_{\cos\alpha}\right)}{\sin 2\phi\cos\phi}\gamma D\right]V \tag{8}$$

$$R_A = \cos\alpha\sqrt{\cos(\alpha+\phi)\cos(\alpha-\phi)}$$

$$R_B = \sin\alpha\sqrt{\sin(\alpha+\phi)\sin(\alpha-\phi)}$$

$$R_C = \frac{\sin 2\alpha + \left({}^{2C}\!/_{D}+1\right)\sin 2\phi}{\cos 2\phi - \cos 2\alpha}$$

$$P_V = \frac{\pi D^2}{4}\left[R_B R_C^2 - R_A\right]\frac{cV}{\sin\phi} \quad (9)$$

$$\sigma_T = \frac{P_V - Pe}{\left(\pi D^2 R_A / 4\cos\phi\right)V} \quad (10)$$

6. Applications

6.1. Single Tunnel

Following the general method described in the preceding section (and with Cu=100, D=5m, γ=20, γD/Cu=1), the collapse stability ratios for tunnels at different depths (i.e. C/D ratios) are obtained. All results (C/D=1, 2, 3, 4) from the Finite Element calculation are compared with the upper The FOS slope can be defined as the ratio of the available shear strength of the soil to that required to maintain equilibrium, Bishop. Where FOS is the factor of safety, N_c is the critical stability ratio, and N_f is the field stability ratio. Case 1, When N_c is greater than N_f, FOS more than one, the tunnel is in a stable state. Case 2, When N_c equals N_f, FOS equals one, a tunnel is stability. Case 3, When N_c is less than N_f, FOS less than one, a tunnel is stability.

Table 2.
Stability ratios by the bounds and EFM

C/D	Nu	Nf	Nl
1	3.35	3	2.7
2	4.52	4	3.64
3	5.44	5	4.28
4	6.22	5.33	4.8
5	6.91	5.65	5.18

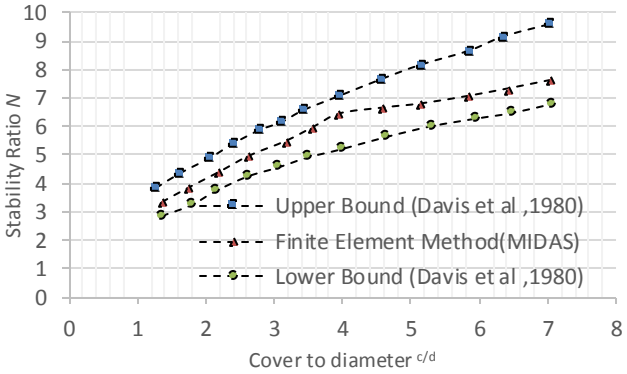

Fig.9. Stability ratios of a single tunnel (γD/Cu=1)

Bound and the lower bound solutions (Davis et al. 1980) in Table 1 and Figure 10: Where Nu is the stability ratio that is an upper bound solution, N_f is the stability ratio that is an upper bound solution by finite element method, N_l is the stability ratio that is the lower bound solution.

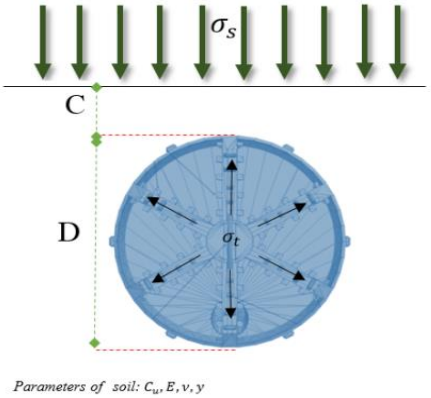

Fig. 10. Single circular tunnel in cohesive soil

6.2. Two Parallel Circular Tunnels with the Same Diameters

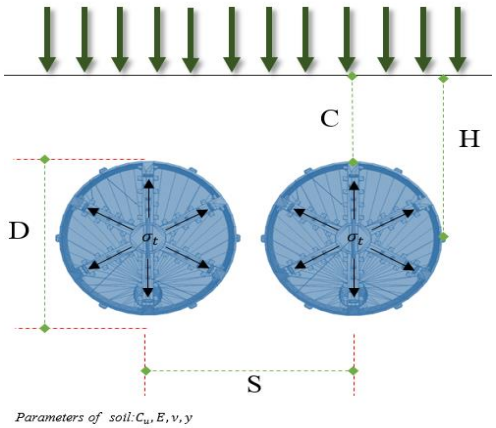

Fig 11. The model of two parallel circular tunnels with the same diameters

Table 3.
The upper bound Nu and lower bound Nl of stability ratios for two tunnels (S/D=0.5)

C/D	1	2	3	4
Nu	3.5	4.2	4.8	5.35
Nl	0.9	1.2	2.7	3.2

Sloan et al theoretical and experimental methods are used to study the untrained stability of a shallow buried circular tunnel in soft soil. The hard boundaries required to resist collapse are obtained using two numerical methods based on the finite element formulation of the classical limit theorem [26].

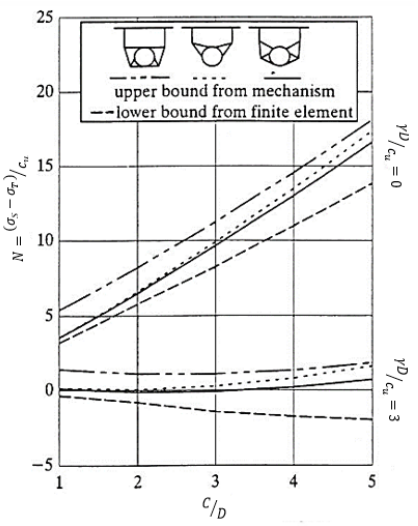

Fig.12. Comparison of stability bounds for the circular tunnel (Sloan et al 1993)

Charles E et al the stability of the strained side of the slab under undrained conditions is investigated using the finite element method. In most cases, improvements to the solution algorithm allow very close boundaries to be drawn, providing useful diagrams for assessing the stability of these types of subsurface openings [27].

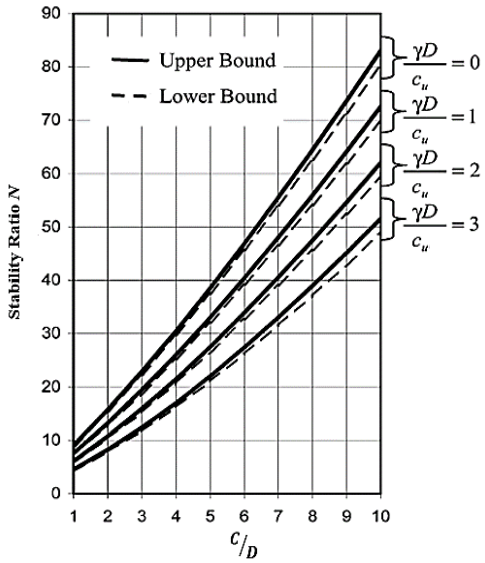

Fig.13. Parameter stability limit equilibrium (Charles E 2003)

Abbo A et al A compact set of stability charts that are useful for design purposes has been generated. In addition, an accurate approximate equation for computing tunnel stability has been found by curve-fitting the finite element limit (ABAQUS) analysis solutions. For the vast majority of cases, this equation will give a slightly conservative prediction of tunnel stability.

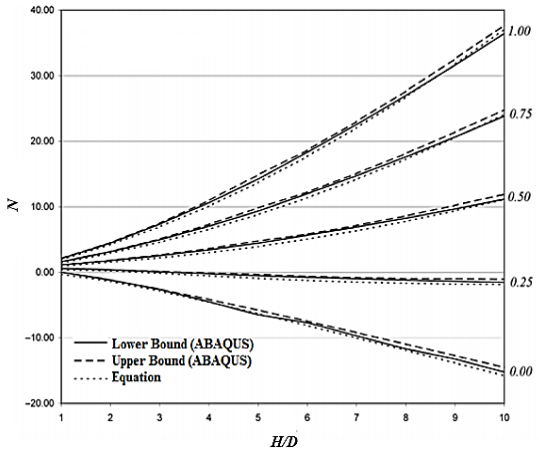

Fig.14. Comparison stability factor of limit equilibrium and design formula using Eqs (Abbo A 2011)

Hui Qi et al. show that the proposed method overestimates the stability numbers for model tests by an average of 2.5% and agrees well with the finite element limit analysis (FELA) results. Methods based on pore shrinkage theory are then discussed, which can provide useful guidance to designers for estimating the stability of shallow tunnels/rankings in clay soils [28].

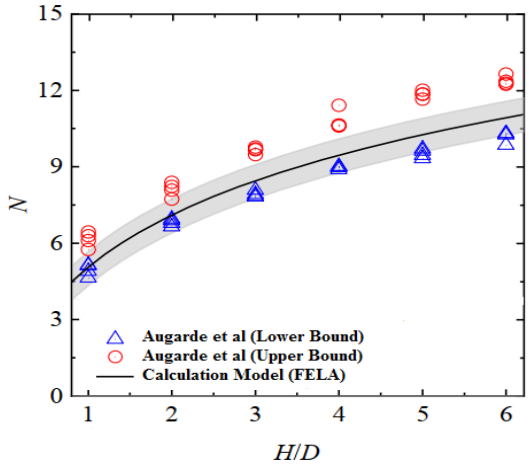

Fig.15. Comparison of predicted stability numbers with FELA results *(*Hui Qi 2021*)*

6.3. The Failure Mechanism for Twin Parallel CircularTunnels with Different Diameters

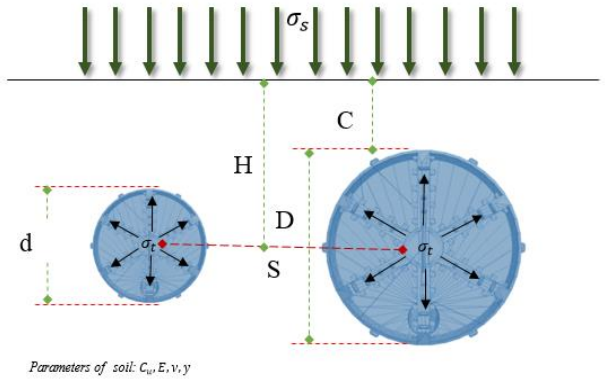

Fig. 16. The failure mechanism of twin parallel circular tunnels with different diameters

Figure 17 shows the critical stability ratios (N_C) of twin parallel circular tunnels with different diameters (D=2d), the larger single tunnel (C/D=1, γD/Cu=0.8, N_C=3.1) and the smaller single tunnel (C/D=2.5, γd/Cu=0.38, N_C=4.6).

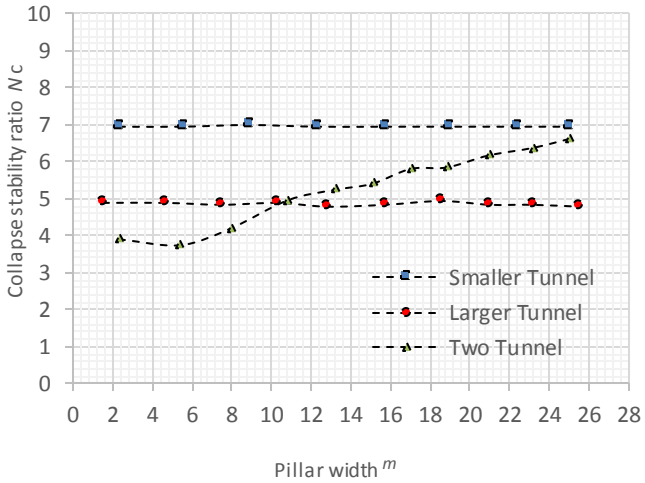

Fig. 17. The critical stability ratios of two tunnels, the larger and smaller tunnels.

The stability ratios for the upper and lower bound are shown in Figure 18, and the stability ratios were compared with the stability ratio solved by the finite element program MIDAS/GTS.

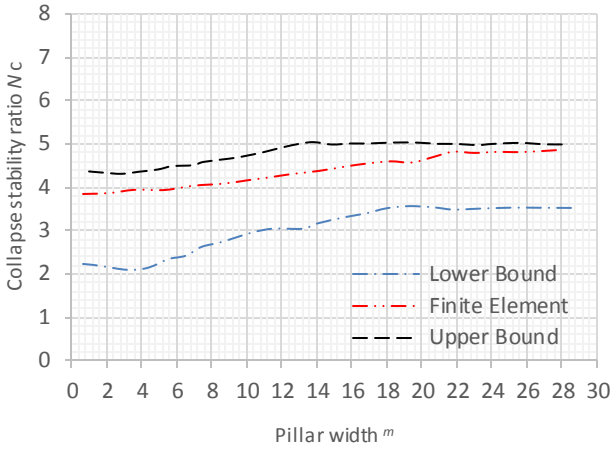

Fig. 18. The tunnel collapse stability ratios of upper, lower bounds solution and finite element solution

7. Discussion

Upper-bound solutions of FOS are derived from the decay and detonation failure mechanisms proposed by Leca and Dormieux. Using the generalized tangential technique, a non-linear failure criterion is introduced into the energy dissipation calculation. The upper bound solution of FOS is compared with the result calculated by the limit equilibrium method. The solution of FOS derived in this paper is almost the same as the solution calculated by the ultimate equilibrium method, proving that the method proposed in this paper is effective. Parametric studies have shown that the parameters m and C/D have a significant influence on the FOS stabilization of the tunnel.

The tunnel stability ratios were obtained by the external force increment method (EFI). Introduced several new concepts including natural stability ratio, field stability ratio, critical stability ratio, stability analysis plane, stability analysis plot, and stability analysis line. The critical stability ratio is a criterion to judge tunnel stability in the stability analysis. There are three ways to arrive critical state that corresponds with the critical stability ratio, which is increasing the unit weight of soil, increasing eternal force, or the reducing supporting force in the tunnel. In hand calculation of the tunnel stability by limit analysis, it is generally difficult to deal with the critical stability ratio. By the EFI, such problems can be treated as easily as problems of a critical

stability state. For practical problems with a critical stability state, EFI would be more advantageous than other methods. A single tunnel, two parallel circular tunnels with the same diameters, and two parallel circular tunnels with different diameters were calculated by the external force increment, the results well corresponding tothe limit analyses method.

8. Conclusion

This paper investigates the relationship between the volume reduction of tunnel linings and the C/D to diameter ratio. Many (empirical) relationships based on the literature, such as the stable number method and the finite element method have been used. Tunnel surfaces should be supported to minimize settlement of the ground ahead of the tunnel and to prevent damage to the soil ahead of the ground. However, the mechanisms that occur during facial collapse are not fully understood. A new method for stability analysis of EFIM clay tunnels is proposed, and a new concept of strength reduction method different from the finite element method and the safety factor is proposed. This method can be used for tunnel stability analysis and is illustrated by three examples. The results of the critical stability ratio of the tunnel obtained by finite element analysis are compared with those obtained by boundary theorem. They are bounded by upper and lower-bound solutions in the limit analysis of plasticity theory. Therefore, this method is usually easier to implement than other methods.

References

[1] Broms, B. B., H. Bennermark. 1967. “Stability of clay atvertical openings”. J. Soil Mech. Found. Div. 1967, 93, 71–94.

[2] Kimura, T., R. Mair.. “Centrifugal testing of model tunnels in soft clay.” In Proc., 10th Int. Conf [C]. On Soil Mechanics and Foundation Engineering, 1981, 319–322. Rotterdam,the Netherlands: A. A. Balkema.

[3] Davis, E. H., M. J. Gunn, R. J. Mair, and H. N. Seneviratne. “The stability of shallow tunnels and underground openings in cohesive material.” Géotechnique, 1980, 30 (4): 397- 416. ttps://doi.org/10.1680/geot.1980.30.4.397.

[4] Wilson, D. W., A. J. Abbo, S. W. Sloan, and A. V. Lyamin. “Undrained stability of a square tunnel where the shear strength increases linearly with depth.” Comput. Geotech, 2013, 49: 314–325. https://doi.org/10.1016/j.compgeo.2012.09.005.

[5] Abbo, A. J., D. W. Wilson, S. W. Sloan, and A. V. Lyamin. “Undrained stability of wide rectangular tunnels.” Comput. Geotech, 2011, 53: 46–59. https://doi.org/10.1016/j.compgeo.2013.04.005.

[6] Shiau, J., and F. Al-Asadi. “Three-Dimensional Analysis of Circular Tunnel Headings Using Broms and Bennermark’s Original Stability Number [J] “. Int. J. Geomech., 2020, 20 (7): 06020015.

[7] Shiau, J., and F. Al-Asadi. “Revisiting Broms and Bennermarks’ original stability number for tunnel headings.” Geotech, 2018, Lett.8 https://doi.org/10.1680/jgele.18.00145.

[8] Shiau, J., and F. Al-Asadi. “Determination of critical tunnel heading pressures using stability factors.” Comput. Geotech, 2020, 119: 103345. https://doi.org/10.1016/j.compgeo.2019.103345.

[9] Shiau, J., and M. M. Hassan. “Undrained stability of active and passive trapdoors.” Geotech. Res, 2019, 7 (1): 40–48. https://doi.org/10.1680 /jgere.19.00033.

[10] Shiau, J., and M. Sams. “Relating volume loss and greenfield settlement.” Tunneling Underground Space Technol, 2019, 83:145–152. https://doi.org/10.1016/j.tust.2018.09.041.

[11] Zienkiewicz O. C., Humpheson C., and Lewis R. W. “Associated and nonassociated visco-plasticity and plasticity in soilmechanics [J] “. Geotechnique, 1975, 25 (4): 671 - 689.

[12] Zhang, Q.; He, W.; Zhang, H.-Y.; Wang, H.-Y.; Jiang, B.-S. “A simple numerical procedure for the elastoplastic coupling finite strain analysis of circular tunnels in strain-softening rock masses“. Comput. Geotech. 2021, 130, 103921.

[13] Broms, B. B., Bennermark, H. “Stability of clay in vertical openings [J]. J. “soil Mech. Found. Div. ASCE. 1967, 193 (SM1): 71-94.

[14] Dawson, E. M., Roth, W. H. and Drescher, “a Slope Stability Analysis by Strength Reduction [J] “. Geotechnique, 1999, 49 (6): 835-840.

[15] Zhang, F.; Gao, Y.F.; Wu, Y.X.; Zhang, N. “Upper-bound solutions for face stability of circular tunnels in undrained clays“. Géotechnique, 2017, 68, 76–85.

[16] S. M. Marandi, M. Anvar, and M. Bahrami, “Uncertainty analysis of safety factor of an embankment built on stone column improved soft soil using the fuzzy logic α-cut technique,” Computers and Geotechnics, vol. 75, pp. 135–144, 2016.

[17] W. Bishop, “The use of the slip circle in the stability analysis of earth slopes,” Geotechnique ´, 1954, vol. 5, no. 1, pp. 7–17.

[18]Xie J., Gunn M., and Rahim, A. Collapse of two parallel circular tunnels with different diameters in soil [C]. The 9th Symposium on Numerical Models in Geomechanics---null

[19]Huang, M.; Li, S.; Yu, J.; Tan, J.Q.W. "Continuous field-based upper bound analysis for three-dimensional tunnel face stability in undrained clay ". Comput. Geotech. 2018**,** 94, 207–213.

[20]J. L. Qiao, Y. T. Zhang, J. Gao et al., "Application of strength reduction method to stability analysis of shield tunnel face, Journal of Tianjin University, 2010, vol. 43, no. 1, pp. 14–20.

[21]X. L. Yang and J. H. Yin, "Slope stability analysis with nonlinear failure criterion," Journal of Engineering Mechanics, 2004, vol. 130, no. 3, pp. 267–273.

[22]Behnen, G., Nevrly, T., Fischer, O.: Bettung von Tunnelschalen (Bedding of Tunnel Linings). Tunnelbau-Taschenbuch2013, DGGT, VGE-Verlag, 2012, pp. 235–282.

[23]Geotechnical Engineering Handbook, 1991, Vol. 1: Fundamentals, Part 1, 4th ed., Ernst & Sohn.

[24]G. Anagnostou and K. Kovari, "Face stability conditions with ´ Earth-Pressure-Balanced shields," Tunnelling and Underground Space Technology, 1996, vol. 11, no. 2, pp. 165–173.

[25]E. Leca and L. Dormieux, "Upper and lower bound solutions for the face stability of shallow circular tunnels in frictional material," Geotechnique, 1990, vol. 40, no. 4, pp. 581–606.

[26]Sloan, S.W.; Assadi, "A. Stability of Shallow Tunnels in Soft Ground"; Predictive soil mechanics. In Proceeding with the Wroth Memorial Symposium, Oxford, UK, 27–29 July 1992; Thomas Telford: London, UK, 1993; pp. 644–663.

[27]C.E. Augarde, Andrei V. Lyamin, S. W. Sloan. "Stability of an undrained plane strain heading revisited". 2003, Computers and Geotechnics 30 -419–430.

[28]Hui Qi, Wenjie Cui, Huaijian Li, Junwei Cheng, Lingdi Kong, Xiaonan Wang, Jianliang Zhang 3, Gongzeng Yang, Hongya Yue, and Xiuguang Song."Undrained Stability Analysis of Shallow Tunnel and Sinkholein Soft Clay: 2021, The Cavity Contraction Method"applied science. *11*, 9059 .https://doi.org/10.3390/app11199059.